Response of the topside ionosphere to recurrent geomagnetic activity

Jing Liu,[1,2,3] Libo Liu,[1] Biqiang Zhao,[1] Weixing Wan,[1] and Roderick A. Heelis[4]

Received 15 June 2010; revised 4 September 2010; accepted 24 September 2010; published 21 December 2010.

[1] In the present study we investigate the solar activity, local time, and latitudinal dependence of the topside ionosphere response to recurrent geomagnetic activity, using 8 years (1998–2005) of data on total ion density (Ni) retrieved from Defense Meteorological Satellites Program observations at about 840 km altitude. It is the first attempt to explore the presence of oscillations in the topside ionosphere in response to recurrent geomagnetic activity. Results indicate that striking periodic oscillations around 9 days in Ni are present during the latter part of the declining phase of solar cycle 23. The percentage of the magnitude of 9 day oscillations relative to background values in Ni at 2130 LT tends to be 5%–10% larger than at three other local times (0930, 0510, and 1710 LT). Moreover, latitudinal profiles of bandpass-filtered 9 day perturbations in Ni show multiple peaks as a function of local time and day of the year, which is distinctly different from previous results at or around the *F*2 layer peak. There are in-phase correlations between *Kp* and the Ni responses in the winter hemisphere and at middle and low latitudes, and approximately anti-phase at high latitude in the summer hemisphere. Additionally, the 9 day oscillations in ion temperature are is mainly restricted to high latitudes. The combined effects of neutral winds, $E \times B$ drift, auroral ionization precipitation, and migration of subauroral trough region are possible candidates to explain the latitudinal profiles of the 9 day variations in Ni.

Citation: Liu, J., L. Liu, B. Zhao, W. Wan, and R. A. Heelis (2010), Response of the topside ionosphere to recurrent geomagnetic activity, *J. Geophys. Res.*, *115*, A12327, doi:10.1029/2010JA015810.

1. Introduction

[2] External energy flow through the Earth's thermosphere and ionosphere and its signature remains a frontier in scientific research. As suggested by *Forbes et al.* [2000] and *Fuller-Rowell et al.* [2000], three energy sources are thought to induce ionospheric or thermospheric variations: (a) the solar ionizing flux; (b) meteorological influences, including planetary waves with typical periods of about 2–30 days in the atmosphere [*Vincent*, 1990; *Xiong et al.*, 2006], which are not expected to propagate upward above 110 km [*Pogoreltsev et al.*, 2007]; and (c) the interactions between the solar wind and the magnetosphere-ionosphere-thermosphere system [*Burke et al.*, 2010]. These sources may disturb the ionosphere-thermosphere, showing considerable periodic variations superimposed on the background state.

[3] In addition to the response of the ionosphere to recurrent geomagnetic disturbances at the well-known period of about 27 days corresponding to solar rotation, a shorter periodic response of 13.5, 9, and 7 days has also been reported [e.g., *Svalgaard and Wilcox*, 1975; *Musman and Altrock*, 1978; *Neugebauer et al.*, 2000; *Nayar et al.*, 2001; *Tsurutani et al.*, 2006]. Periodicities of 7 and 9 days are found to exist in the *Kp* index and are linked to the periodic appearance of solar coronal holes and their associated high-speed solar winds [*Nayer et al.*, 2001; *Tsurutani et al.*, 2006; *Temmer et al.*, 2007]. Through comparison among the temporal evolution of coronal hole areas, interplanetary parameters, and the geomagnetic index, *Temmer et al.* [2007] found that the triangular distribution of coronal holes about 120° apart in longitude leads to periodic variations in the solar wind and recurrent geomagnetic activity. High-speed streams from coronal holes will overtake and compress upstream low-speed solar winds from helmet streamers or their boundaries [*Nerney and Suess*, 2005], forming corotating interaction regions (CIRs) [*Tsurutani et al.*, 2006]. When CIRs impinge on the Earth, they induce moderate recurrent geomagnetic activity that persists for several days or even for up to the entire solar rotation [*Tsurutani et al.*, 1995; *Denton et al.*, 2006; *Shugai et al.*, 2009].

[4] It is well established that the source region of the high-speed solar wind stream changes with the solar cycle, moving toward the solar equator from the polar regions at solar minimum and retreating into the polar regions and becoming much less frequent around solar maximum [*Krieger et al.*, 1973; *Mursula and Zieger*, 1996; *Harvey et al.*, 2002;

[1]Beijing National Observatory of Space Environment, Institute of Geology and Geophysics, Chinese Academy of Sciences, Beijing, China.
[2]Also at State Key Laboratory of Space Weather, Chinese Academy of Sciences, Beijing, China.
[3]Also at Graduate University of the Chinese Academy of Sciences, Beijing, China.
[4]Hanson Center for Space Sciences, University of Texas at Dallas, Richardson, Texas, USA.

0148-0227/10/2010JA015810

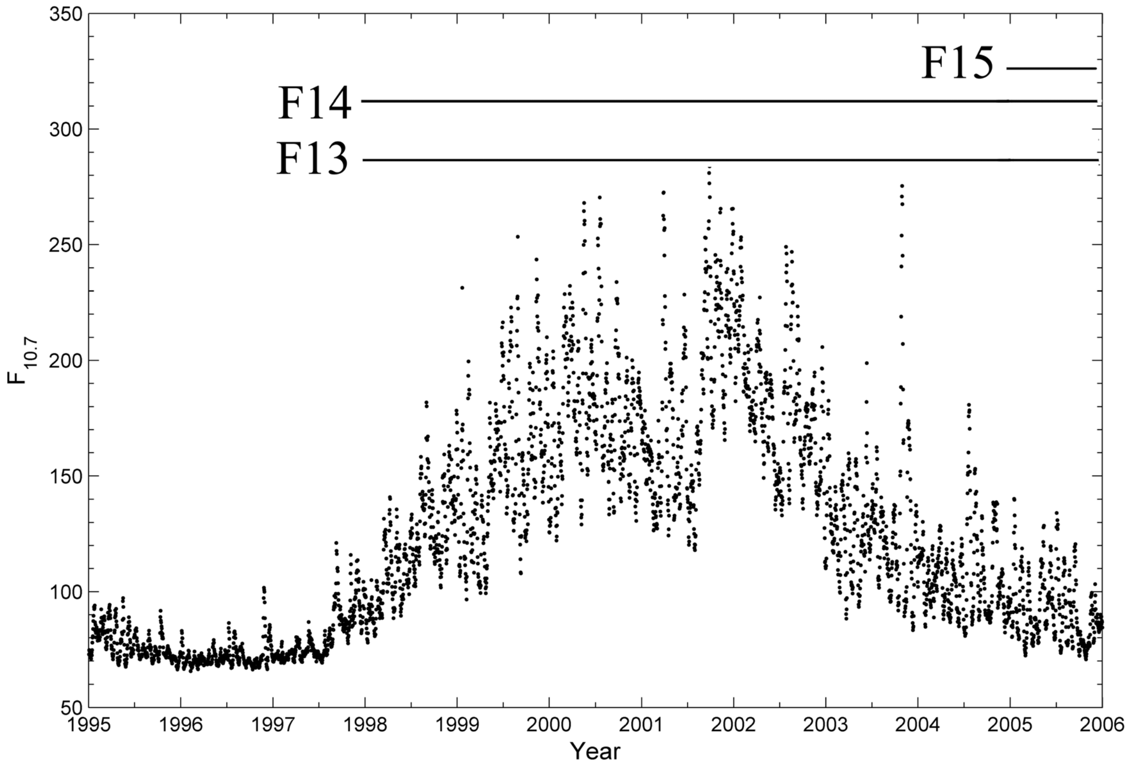

Figure 1. Time coverage of the Defense Meteorological Satellites Program (DMSP) Ni we used and variations of solar index $F_{10.7}$ (in units of 10^{-22} W m^{-2} Hz^{-1}) during 1995–2005.

Tsurutani et al., 2006]. In contrast, coronal mass ejections (CMEs), the driver of nonrecurring geomagnetic activity, are more likely to occur at solar maximum [*Borovsky and Denton*, 2006; *Denton et al.*, 2006]. The durations linked to CMEs are unusually shorter than CIRs. Hence, the solar activity dependence of the two dominant drivers of magnetospheric disturbances determines the recurrence rate of geomagnetic activity. Using the thermosphere densities at 400 km altitude from CHAMP observations during the descending phase of solar cycle 23 (2002–2007), *Lei et al.* [2008a, 2008b] found periodic oscillations of about 7 and 9 days in thermospheric density related to high-speed streams, and these periodic variations in the thermosphere tend to occur during the later part of this descending phase. Unfortunately, the solar activity dependences of the periodic oscillations in the ionosphere and associated recurrent geomagnetic activity have not been extensively studied.

[5] Recently, a solar-terrestrial connection has been elucidated among open-field coronal holes, high-speed solar wind streams, enhanced geomagnetic activity, and modifications in the thermosphere-ionosphere during the latter part of solar cycle 23 [*e.g.*, *Crowley et al.*, 2008; *Lei et al.*, 2008a, 2008b, 2008c, 2010; *Mlynczak et al.*, 2008; *Thayer et al.*, 2008; *Zhang et al.*, 2010]. *Lei et al.* [2008a, 2008c] discovered that coronal holes rotating with the Sun induce a 9 day periodic variation of the solar wind, the geomagnetic activity, and the thermospheric neutral density as well as the ionospheric total electron content (TEC). The changes in thermospheric and ionospheric parameters in reaction to recurring geomagnetic forcing depend on latitude, local time, and season. *Lei et al.* [2008a] and *Thayer et al.* [2008] demonstrated that the thermospheric density shows ±20%–30% perturbations from background levels. Additionally, *Crowley et al.* [2008] revealed that the change in the ∑O/N2 ratio associated with the 9 day recurrent geomagnetic activity is larger (±15%–20%) at higher latitudes than at lower latitudes (±5%). *Pedatella et al.* [2010] pointed out that nighttime 9 day TEC oscillations concentrated at higher latitudes are close to ±40% of the background level, while the maximum variations (±25%) in daytime TEC occur at midlatitudes. Although there are only moderate geomagnetic activity levels associated with CIRs and high-speed solar winds with periods of 7 and 9 days, the cumulative effects may impact the state of the ionosphere-thermosphere for several days up to weeks [*Thayer et al.*, 2008].

[6] Evidence shows that the plasma density at different heights behaves in somewhat different ways during geomagnetic disturbances. For example, *Tulasi Ram et al.* [2010] found that the density perturbations based on the Constellation Observation System for Meteorology, Ionosphere, and Climate (COSMIC) observations at low latitudes are generally in phase with *Kp* above the *F*2 peak and out of phase below the *F*2 peak. Using measurements of COSMIC vertical TEC in the altitude range of roughly 800 and 20,200 km, *Pedatella and Larson* [2010] elucidated that the plasmapause oscillates with periods of 9 and 13.5 days in the year 2008 in association with recurring geomagnetic activity due to high-speed solar streams. As a transition region from the plasmasphere to the lower ionosphere, the signatures of recurrent geomagnetic activity in the topside ionosphere, for example, at a height of about 840 km, are yet to be known.

[7] In addition to the aforementioned altitude dependence of the ionospheric response to recurrent geomagnetic activity, the ionospheric plasma density also experiences somewhat different variations at different local times. For instance, the low-latitude disturbance electric fields and plasma drifts during the period of one or a few days after geomagnetic disturbance conditions are generally due to ionospheric disturbance dynamo electric fields resulting from enhanced auroral heating [*Blanc and Richmond*, 1980]. These perturbed electric fields are westward during the day and eastward at night.

[8] The objective of this study is to investigate the latitudinal and local time variation of the response in the topside ionosphere to recurrent geomagnetic activity using the series of Defense Meteorological Satellites Program (DMSP) satellite observations. The solar activity dependence of the multiday oscillations in interplanetary parameters, geomagnetic *Kp* index, and topside Ni are also compared.

2. Data Set and Analysis Methods

[9] In situ measurements of solar wind speed by the ACE satellite are used to investigate its spectral variations during the years 1998–2005. The DMSP spacecraft are in a near-polar, Sun-synchronous orbit, at a constant geocentric altitude of ~840 km. Since 1987, a series of DMSP spacecraft has been launched, designated with the letter F and the flight numbers. The orbit period is about 101 min, and consecutive orbits are separated in longitude by about 25.5°. The nearly constant local time of DMSP orbits at middle and low latitudes makes their ionospheric measurements unique for allowing other drivers of plasma characteristics to be more noticeable.

[10] The data we used are provided from the observations of the F13, F14, and F15 satellites whose orbits cross the geographic equator at approximately 1710/0510, 2030/0830, and 2130/0930 LT, respectively. The time coverage and the corresponding 10.7 cm solar flux, $F_{10.7}$, are illustrated in Figure 1. In this study, data from the University of Texas, Dallas, Web site provide the total ion concentration (Ni) and the ion temperature (Ti) obtained separately from the scintillation meter and the retarding potential analyzer (RPA), with a 4 s resolution.

[11] At high latitudes the sampling local time deviates from the equatorial crossing local time, so we only present DMSP data between ±60° magnetic latitudes (MLAT). As indicated in Figure 1 of *Zhao et al.* [2005a], there is a difference of almost an hour in local time between the midlatitude Northern Hemisphere data and the midlatitude Southern Hemisphere data. The combination of the data from both hemispheres is reasonable if we consider that the topside ionosphere changes are not very dramatic 1–2 h after sunset and before noon [*Macpherson et al.*, 1998].

3. Results

3.1. Solar Activity Dependence of Period Variations in the Solar Wind, Geomagnetic Activity, and Topside Plasma Densities

[12] Figure 2 shows the Lomb-Scargle (L-S) normalized periodogram [*Lomb*, 1976; *Scargle*, 1982] of $F_{10.7}$, solar wind speed, *Kp* index, and orbit-averaged topside ionospheric Ni at 0830 and 2030 LT measured by F14. Each ascending and descending part of the orbit within ±60° magnetic latitudes is averaged separately. L-S periodogram analysis is a least-squares spectral analysis method that estimates frequency spectra based on a least-squares fit of sinusoids to data samples, and spectral amplitudes are normalized by variance. Since the L-S spectral content in Ni is quite similar at different local times (not shown here), observations of Ni from DMSP F14 over 8 years (1998–2005) are used to investigate the solar activity dependence of the multiday oscillations in the topside ionosphere on recurrent geomagnetic activity.

[13] It is shown in Figure 2a that variations in solar wind speed with a 9 day period are strongest in 2005, moderate in 1998, 2000–2002, and 2004, and weaker in 1999 and 2003. This result is in good agreement with *Temmer et al.* [2007], highlighting that the 9 day period is not a singular phenomenon present only around the solar minimum but also occasionally occurs during the maximum and decay phase of solar cycle 23. In contrast, this 9 day periodicity does not appear in the *Kp* index in 2002 and 2003, indicating that at this time the solar wind speed alone cannot represent the total magnetospheric energy input [*Lei et al.*, 2008b]. The correlation coefficients between neutral density oscillations and *Kp* perturbations are much larger than those between neutral density and solar wind speed during the years 2002–2007. The CIR-generated geomagnetic storms are mainly attributed to the southward components of high-amplitude Alfven waves within the body of the corotating streams [*Tsurutani et al.*, 1995]. In the topside ionosphere, Ni variations show prominent peaks at 9 days in 2004 and 2005 but a weaker response in other years (1998–2003). As depicted in Figure 2b the 9 day periodicity existing in ion temperature shows solar activity dependence similar to that of the same period in topside ionospheric Ni. The 9 day oscillation in Ti is not as pronounced as that in plasma density and most of the spectral amplitude for 9 day oscillation is below the 95% confidence level.

[14] In short, a 9 day periodic variation in solar wind speed is present during the solar maximum (2000 and 2001) and during the declining phase (2004 and 2005). However, the response of *Kp* and the topside ionospheric density to the solar wind is pronounced only during the declining phase. During the solar maximum the ambient solar wind flow is interrupted by CMEs, breaking the direct relation between the appearance of coronal holes and recurrent geomagnetic activity [*Tsurutani et al.*, 2006; *Lei et al.*, 2008b]. In this way the 7 and 9 day periodicities are not evident in the *Kp* index during the solar maximum (2002–2003). Meanwhile, the topside ionospheric Ni oscillates with a 9 day period only during the latter part of the descending phase of solar cycle 23. This suggests that periodic variations in solar wind speed and related geomagnetic activity are not the only drivers of ionospheric variations. Other influences, such as solar radiation and dynamic drivers from below, may be superimposed on the straightforward relationship between the energy input from the magnetosphere and the ionospheric response.

[15] In addition to the aforementioned 9 day recurrence in solar wind speed and *Kp* index, a 13.5 day period variation sometimes appears in the driver and in the response during the years from 2000 to 2004. This suggests that the occur-

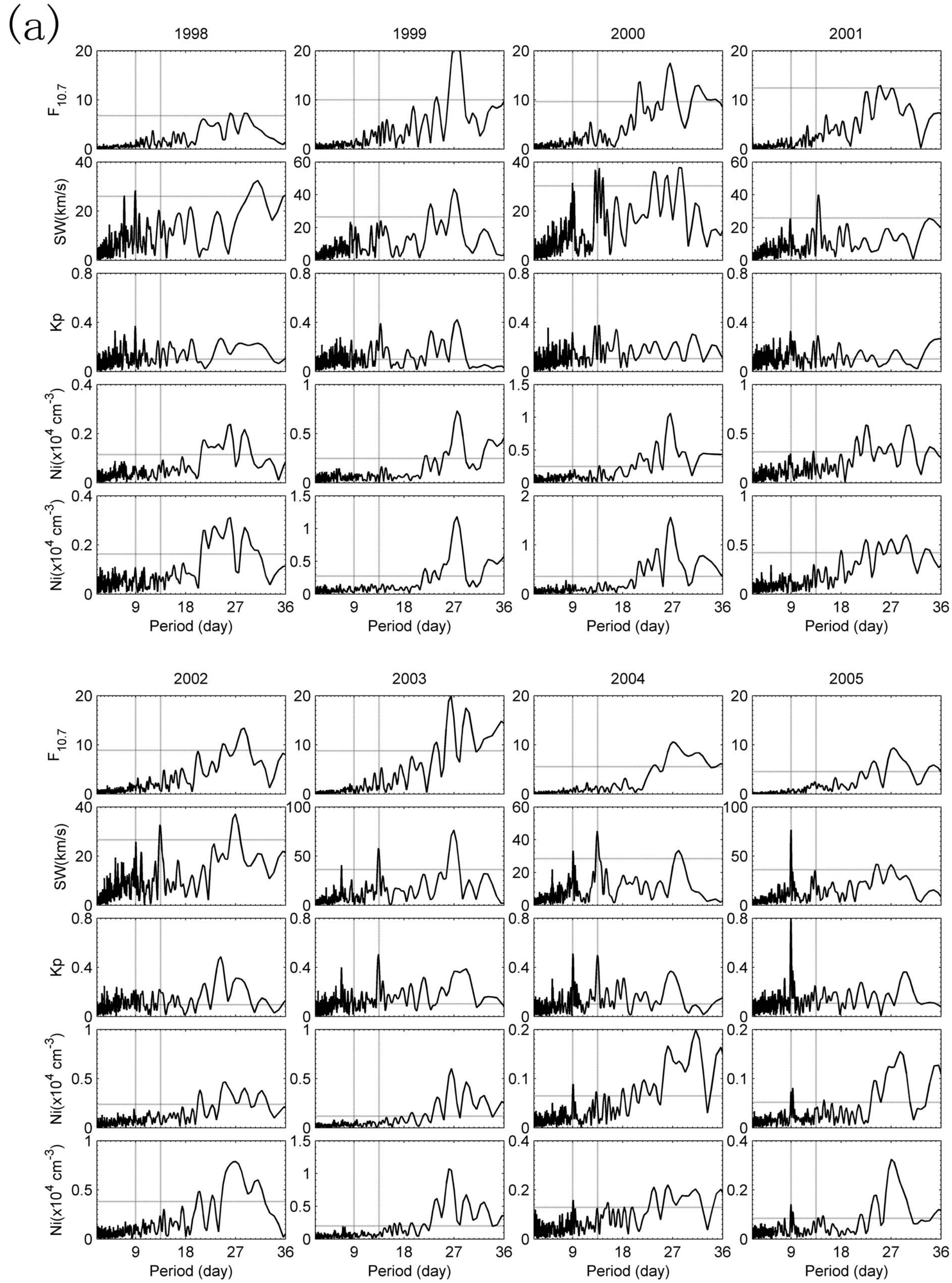
(a)
1998
1999
2000
2001
2002
2003
2004
2005
$F_{10.7}$
SW(km/s)
Kp
Ni($\times 10^4$ cm^{-3})
Ni($\times 10^4$ cm^{-3})
Period (day)

Figure 2

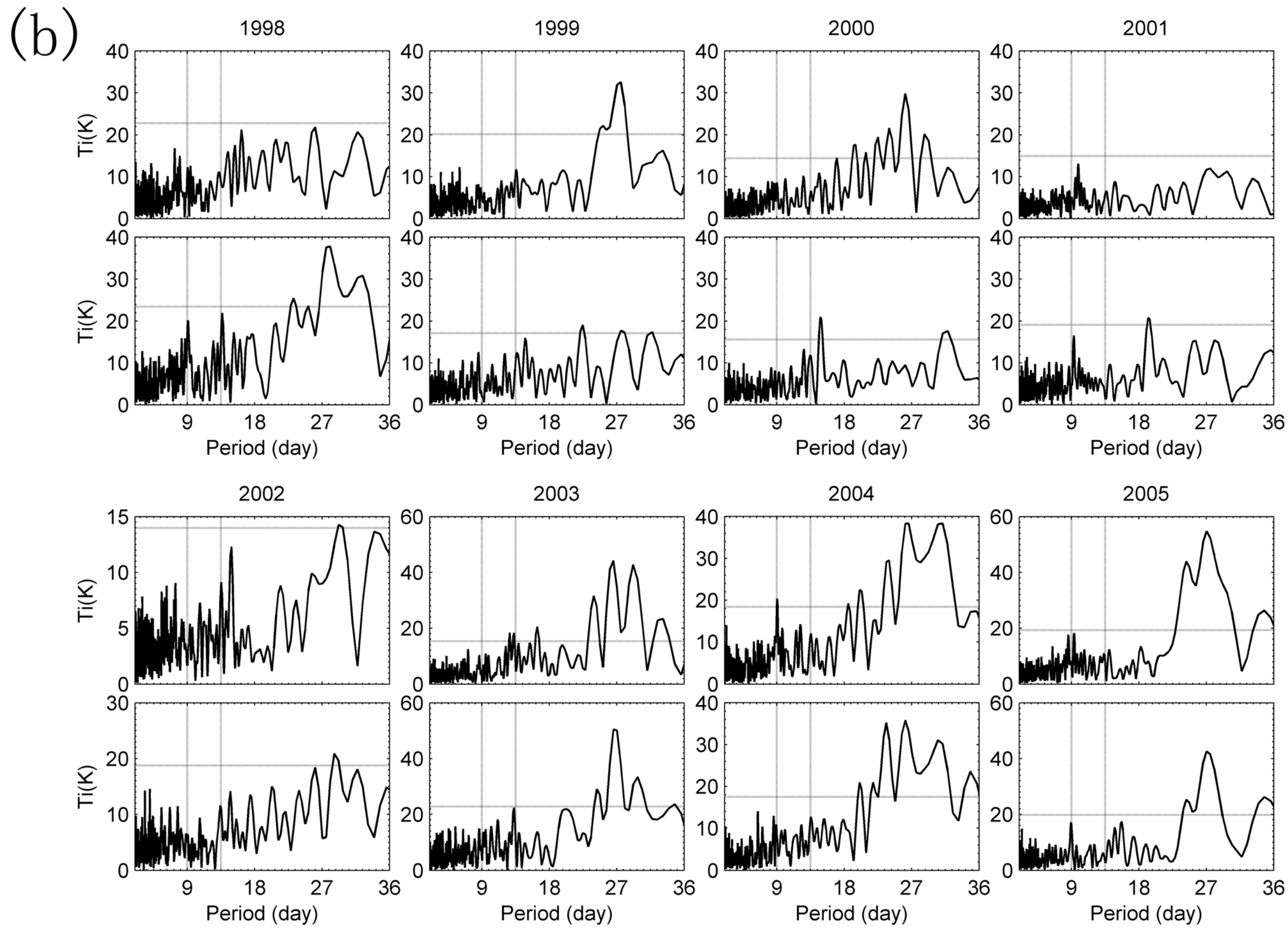

Figure 2. (continued)

rence of a 13.5 day period is not limited to solar minimum periods but also appears during solar maximum. However, the response in *Kp* and in the topside ionospheric density again appears to be most prominent in the declining phase of the solar cycle. This result expands on the finding by *Mursula and Zieger* [1996] that the 13.5 day period at Earth was found predominantly during the solar minimum, owing to the occurrence of two high-speed solar wind streams per solar rotation. Alternatively, *Bobova and Stepanina* [1994] suggested that a 13.5 day period is due to similar periodic variations in the solar chromospheres occurring mainly around solar cycle maxima. The same 13.5 day periodicities are also observed in the X-ray, extreme ultraviolet, and ultraviolet [*Donnelly and Puga*, 1990; *Hocke*, 2008; *Liang et al.*, 2008]. As a result, we cannot isolate the contributions of the periodic solar ionization oscillation to similar periodic variation in the topside ionosphere from recurring high-speed streams. Hence, in a follow-up investigation we will focus on the 9 day periodicity in the topside ionosphere associated with recurring geomagnetic forcing seen in 2005.

3.2. Local Time and Latitudinal Dependences of the Topside Ionospheric Response to Recurrent Geomagnetic Forcing

[16] Figure 3a presents the latitudinal variation of the topside ionospheric Ni in the year 2005 at 0510 LT; the corresponding L-S periodogram is shown in Figure 3b. As shown in Figure 3a the topside Ni at most latitudes shows a pronounced seasonal asymmetry with higher values in summer than in winter, whereas topside total ion densities in the equatorial regions are higher around the December solstices than the June solstices, which is consistent with the investigations by *Zhao et al.* [2005a] and *Liu et al.* [2007a]. Hemispheric asymmetries are produced by interhemispheric

Figure 2. (a) Lomb-Scargle (L-S) spectral amplitudes of solar index $F_{10.7}$ (in units of 10^{-22} W m^{-2} Hz^{-1}), solar wind velocity, *Kp* index, and DMSP F14 plasma density. The fourth and fifth panels are for the orbit-averaged densities at 0830 and 2030 LT, respectively. The horizontal dashed lines denote the 95% significant level, the vertical dashed lines represent 9 and 13.5 day periods. (b) L-S spectral analysis of DMSP F13 ion temperature during 1998–2005. The first and second panels for each year are for the orbit-averaged Ti at 0510 and 1710 LT, respectively. The horizontal dashed lines denote the 95% significant level; the vertical dashed lines represent 9 and 13.5 day periods.

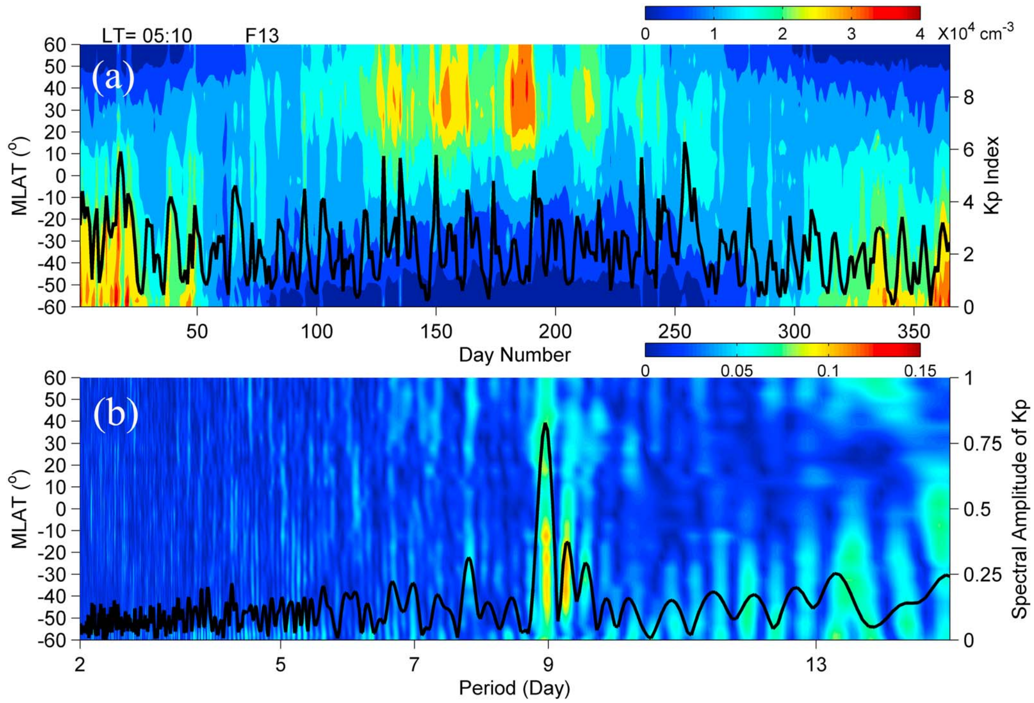

Figure 3. (a) Topside plasma density variations at 0510 LT as a function of magnetic latitude and day in 2005; the daily averaged Kp index is superimposed. (b) Contour plot of normalized spectral amplitudes of DMSP F13 plasma densities (in units of 10^4 cm^{-3}) as a function of magnetic latitude (MLAT) and period in 2005 and L-S periodogram of *Kp* index in 2005 is also superimposed.

neutral winds that lift upward or downward of the *F* region in the summer or winter hemisphere, and thus the topside ionosphere at a fixed height senses an increase or decrease in plasma density [*Rishbeth*, 1998]. As a result, topside Ni has a larger value in the summer hemisphere than in the winter hemisphere. The hemispheric asymmetry in the *F*-peak density also induces field-aligned flows [e.g. *Heelis et al.*, 1990; *Venkatraman* and *Heelis*, 2000], which influence the Ni latitudinal structure in the topside ionosphere [*Greenspan et al.*, 1994; *Watanabe et al.*, 1995; *Sultan and Rich*, 2001]. In addition to the hemispheric asymmetries, a quasi 27 day variation in Ni can be seen in Figure 3a, which is in accordance with the study by *Rich et al.* [2003]; the same feature also exists in TEC [e.g., *Liu et al.*, 2009].

[17] To investigate further the latitudinal dependence of shorter-period variations, less than 15 days, the L-S normalized periodogram of Ni in Figure 3b shows the spectral amplitude of variations in Ni at 0510 LT for the entire year 2005. A predominant spectral peak is found at a period of 9 days at all latitudes and local times covered by the DMSP during this analysis period. The periodograms for other local times are not shown here. This peak is strongly correlated with the same spectral peak in the *Kp* index (black curve), consistent with the earlier observation by *Lei et al.* [2008c] of periodic oscillations in the ionosphere at sub-harmonics of a solar rotation that are linked to the recurrence of geomagnetic activity.

[18] Figure 4 illustrates the latitudinal normalized L-S spectral magnitude variations in Ni with a 9 day period at four local times. The amplitude of the 9 day periodicity varies with latitude with two peaks around MLAT ±30° at 0510 and 0930 LT. A single peak is seen near the magnetic equator at 2130 LT, while at 1710 LT the equatorial peak is accompanied by shoulders at ±30° MLAT. Weak-penetration electric fields from high latitudes will be most effective in the evening sector [*Fejer and Scherliess*, 1997]. In the topside ionosphere, weak upward drift will enhance the ion density at the equator at 2130 LT, without a significant signature of the equatorial anomaly. At the same time,

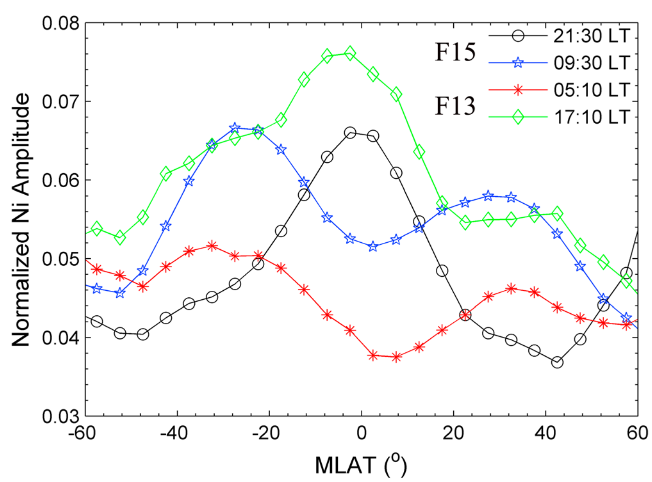

Figure 4. Latitudinal variations of normalized L-S spectral magnitude of the 9 day oscillations in Ni (in units of 10^4 cm^{-3}). Different line colors represent different local times.

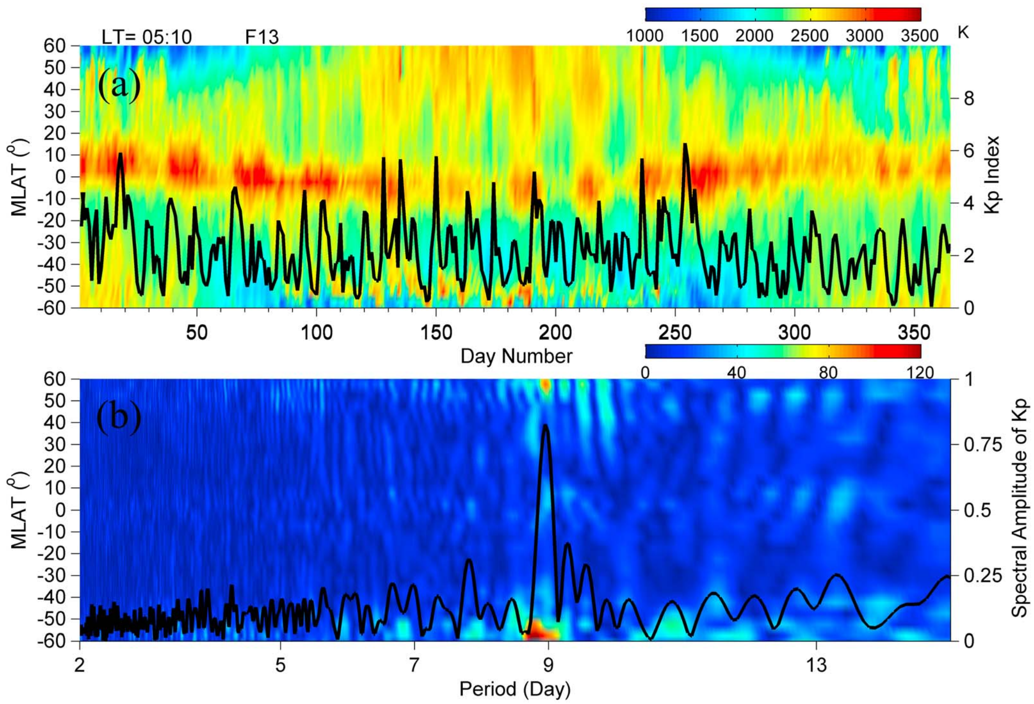

Figure 5. (a) Topside ion temperature at 0510 LT as a function of magnetic latitude and day in 2005; the daily averaged *Kp* index is superimposed. (b) Contour plot of normalized spectral amplitudes of DMSP F13 ion temperature (in units of K) as a function of magnetic latitude and period in 2005; L-S periodogram of *Kp* index in 2005 is also superimposed.

auroral heating will produce equatorward winds that will have their maximum effect at middle latitudes at 1710 LT when the ionosphere is sunlit. In our opinion, the two peaks at 0510 LT should be formed by the same mechanism that explains the two peaks at 0930 LT, since the locations of the two peaks are almost identical where the enhanced equatorward winds reach the maximum effects. The spectral amplitude difference between 0510 and 0930 LT may be caused by different solar ionization intensities and wind fields at these two local times.

[19] Further evidence for the presence of recurrent auroral heating is shown in Figure 5a. A salient feature in Figure 5a is the periodic enhancement of ion temperature at low and equatorial latitudes. We believe that this phenomenon is mainly caused by the same period, with variations of about 27 days in the solar ionization. *Rich et al.* [2003] demonstrated that plasma temperature in the middle- to low-latitude ionosphere at 840 km varies with a period of 27 days, synchronized with the same variation in the $F_{10.7}$ index. It should be noted in Figure 5b that the 9 day oscillation in ion temperature (Ti) appears mainly at middle to high latitudes (50°–60°) and becomes very weak at other latitudes in the year 2005, masked by the influence of solar ionization variations. During periods of enhanced geomagnetic activity the ion temperature tends to increase at high latitudes, and no evident changes take place at low and equatorial latitudes [e.g., *Zhao et al.*, 2005b; *Kil et al.*, 2003]. Using ionospheric temperature measurements made by the Poker Flat Incoherent Scatter Rader during the International Polar Year, *Sojka et al.* [2009] found that CIR events show a one-to-one correlation with ionospheric heating events in both auroral and polar regions.

[20] As depicted in Figure 5b the spectral amplitudes of the ion temperature show asymmetry in the Southern and Northern Hemispheres. The L-S periodogram around 9 days at high latitudes in the Southern Hemisphere is stronger and sparser than in the Northern Hemisphere. The discrepancies in the periods around 9 days between high latitudes in the Southern and Northern hemispheres and *Kp* index are expected to be caused by different energy inputs from the magnetospheres. It was recently reported by *Luan et al.* [2010] that during low and moderate geomagnetic conditions, there are hemispheric energy deposition differences in the local summers between the two hemispheres and, also, the winter-summer asymmetry. The different energy inputs into both hemispheres will lead to different shapes of Ti spectra at high latitudes. Figure 6 shows the latitudinal normalized L-S spectral magnitude variations in Ti with a 9 day period at four local times. This result is distinct from the Ni variations in that the Ti amplitude peaks are restricted to high-middle latitudes at these four local times.

[21] It has been established that 9 day periodicity exists in the topside ionospheric Ni. To acquire more specific information regarding the latitudinal and local time responses to 9 day periodic variations in the topside ionosphere and their relationship to geomagnetic activity, a bandpass filter centered at 9 days, with half-power points at 6 and 12 days, was applied to each magnetic latitude bin (with a window of 5°) of raw Ni and *Kp* index. This bandpass filter is used to extract the 9 day oscillation in plasma density and *Kp*. The percentage differences between the Ni in the bandpass and

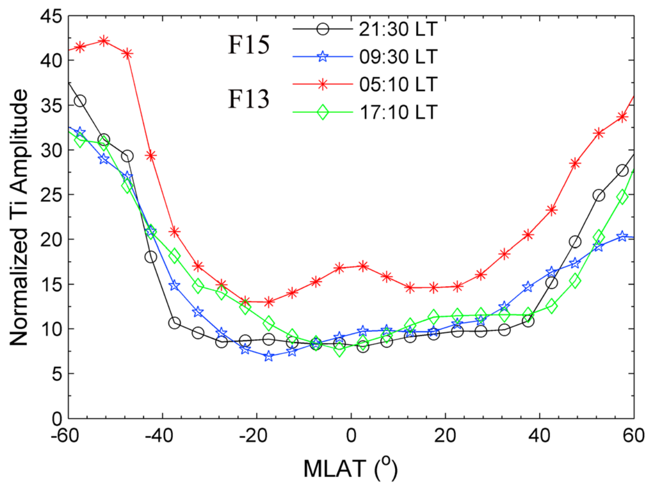

Figure 6. Latitudinal variations of normalized L-S spectral magnitude of the 9 day oscillations in Ti (in units of K). Different line colors represent different local times.

the 11 day running mean are presented in Figure 7 as a function of MLAT and day number. The same method was also applied to thermospheric density by *Lei et al.* [2008a].

[22] In Figure 7 there are clear differences in latitudinal structure of the bandpass-filtered Ni responses at different local times. The largest increases are ~±20% of background levels at 2130 LT and they appear not only at high-middle latitudes (45°–60°) in the winter hemisphere but also at low and equatorial latitudes, which differ from the TEC and CHAMP Ne [e.g., *Pedatella et al.*, 2010]. The bandpass-filtered 9 day perturbations in Ni at high-middle latitudes (50°–60°) in summer and equinox are out of phase with the bandpass-filtered *Kp* perturbations, and they become almost in phase in winter. Generally, the response at the other three local times is ~5%–10% smaller in magnitudecompared to that at 2130 LT.

4. Discussion

[23] The response of the upper ionosphere to recurrent magnetic activity shows quite different behaviors in different seasons, at different local times, at different heights, and at different latitudes. Although there are some similarities between the results reported herein for periodic oscillations of Ni at the height of about 840 km, for electron density variation at about 400 km, and for TEC variations [*Pedatella et al.*, 2010], there are also significant differences.

[24] In Figure 7, at high-middle latitudes in the Southern (summer) Hemisphere at 2130 LT, negative and positive Ni perturbations are nearly opposite in phase from bandpass-filtered *Kp* residuals. A similar anticorrelation between the *Kp* index and TEC in the Southern Hemisphere was discovered by *Pedatella et al.* [2010]; they attributed this phenomenon indirectly to neutral atmosphere composition changes. A similar mechanism may also be responsible for the observed changes in the ionosphere at 840 km in the high-latitude Southern Hemisphere. The composition changes, characterized by enhanced $[N_2]/[O]$ due to upwelling, increase the loss rate and lead to a decrease in electron content, resulting in a

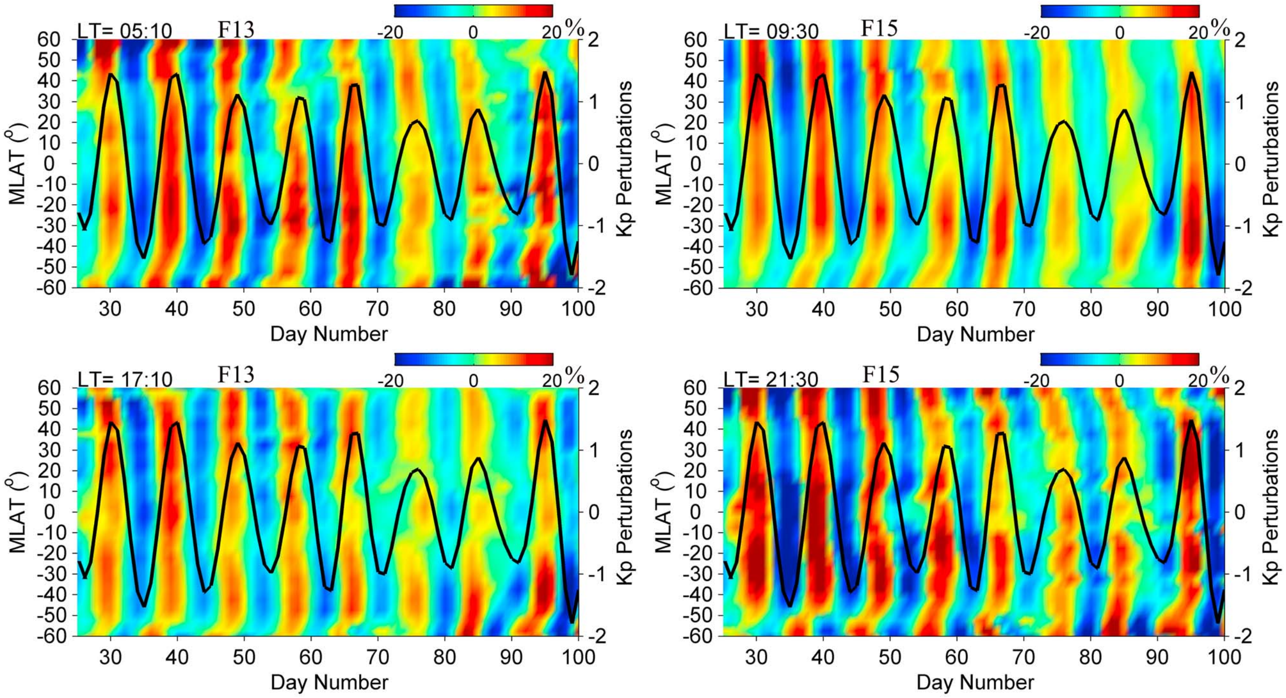

Figure 7. Bandpass-filtered Ni residual as a percentage of the 11 day running mean during days 25–100, 2005. The bandpass filter was centered at a period of 9 days, with half-power points at 6 and 12 days. The perturbations in *Kp* obtained from the same bandpass filter are superimposed (solid black line, right-hand scale).

decrease in Ni in the topside ionosphere. It should be mentioned that the regions of enhanced Ni should be considered as relative enhancements that occur owing to the removal of an 11 day mean value. *Crowley et al.* [2008] have previously pointed out that the ∑O/N2 ratio effect is opposite in phase from *Kp* and is most remarkable at high latitudes, consistent with the results presented here. It should be noted that the antiphase correlation between the ∑O/N2 ratio and the *Kp* index only works at high latitudes. However, the thermospheric mass density oscillates globally [*Qian et al.*, 2010] and is in phase with *Kp*, showing little difference between high and low latitudes [*Lei et al.*, 2008a, 2008b]. Thus we might expect other dynamical processes to be responsible for in-phase correlations between the *Kp* and the topside total ion concentration in the winter hemisphere and at middle and low latitudes.

[25] At 2130 LT, Ni perturbations at high latitudes in the Northern Hemisphere (winter) are approximately in phase with bandpass-filtered *Kp* residuals. This feature was also observed in TEC oscillations by *Pedatella et al.* [2010]. They attributed enhanced auroral particle precipitation and equatorward migration of the wintertime subauroral trough to this phenomenon [*Field and Rishbeth*, 1997].

[26] Equatorward neutral winds, produced by increased auroral energy input, push the plasma upward along magnetic field lines and increase Ni in the topside. For a constant wind this process is most effective for a 45° dip angle owing to the resulting vertical ion motion, $V = W\sin I\cos I$, with I being the dip angle. Such a wind might appear to be delayed by only a few hours with respect to the peak in *Kp*. At middle latitudes a drift perpendicular to the magnetic field in the magnetic meridian will also have a vertical component [*Heelis and Coley*, 2007]. However, that drift's component decreases with latitude, making it less effective at middle and high latitudes. At night, enhanced equatorward neutral winds increase the *F*-layer height at middle to low latitudes without significantly affecting the *F*-layer peak density owing to lack of ionization. However, in the dayside an elevated *F*-layer height due to enhanced neutral winds can increase the *F*-layer peak density and height (hm*F*2). Thus these two mechanisms become most plausible to explain the observed density peak values at middle latitudes.

[27] At low and equatorial latitudes, other sources related to neutral winds and electric fields may contribute to the peak value of Ni. A disturbance dynamo electric field produced by changes in the thermospheric circulation due to periodic variations of joule and particle heating at high latitudes may alter the structure of Ni distributions at low and equatorial latitudes [*Blanc and Richmond*, 1980]. A disturbance dynamo electric field with an eastward polarity can drive the plasma upward and lead to an enhancement of the topside equatorial-low latitude Ni, so the correlation between the density enhancement and the upward vertical drift is very strong [*Heelis and Coley*, 2007].

[28] According to the study by *Tulasi Ram et al.* [2010], the oscillations in hm*F*2 are global and are well in phase with *Kp* variations, indicating that the ionosphere undergoes periodic expansion and contraction as a result of recurrent geomagnetic forcing. At the same time, enhanced energy deposited into polar and auroral regions will lead to an increase in the plasma temperature [*Sojka et al.*, 2009] and a resultant increase in plasma scale height [*Tulasi Ram et al.*, 2010]. The topside plasma density changes are related not only to the changes in neutral winds, neutral composition, temperature, and electric field, but also to their resultant variations in hm*F*2 and scale height [*Liu et al.*, 2007b]. At an altitude of 840 km the plasma density increases because of an increase in scale height and hm*F*2.

[29] The response in the topside ionosphere to recurrent geomagnetic activity is quite small and the specific latitudinal structure depends on the relative importance of these different drivers at different latitudes. However, they all act within a few hours of the response in *Kp* and all produce an in-phase correlation with *Kp*. Further simulations are required to interpret the observed results owing to the lack of simultaneous observations of all necessary parameters.

5. Conclusion

[30] This is the first study to address the solar activity, latitudinal, and local time dependence of the topside ionospheric response at a height of about 840 km to 9 day periodic geomagnetic activity associated with high-speed solar wind forcing using the 8 year data set from DMSP observations. The main results are as follows.

[31] 1. The 9 day oscillations in Ni tend to occur during the latter part of the declining solar cycle, in agreement with the earlier conclusions of *Lei et al.* [2008b].

[32] 2. The latitudinal variation of the amplitude of the 9 day periodicity in ion density response to recurrent geomagnetic activity is quite different from that derived from GPS TEC, CHAMP in situ electron density measurements, and thermospheric response. Our results show peaks in Ni oscillations with a 9 day period, located at high (50°–60°) and low (15°–35°) latitudes), depending on the local time and day of the year. Previous investigations demonstrated that the thermosphere responds to recurrent high-speed streams more strongly at high latitudes than at low latitudes [e.g., *Crowley et al.*, 2008; *Lei et al.*, 2008a]. The combined effects of neutral winds, $E \times B$ drift, expansion of the subauroral trough region, and auroral ionization precipitation may explain the Ni variations that are in phase with the variations in *Kp*. Changes in thermospheric composition are required to produce changes in Ni at summer high latitudes that are out of phase with *Kp*.

[33] 3. This is the first report to show that the topside ionospheric Ti response to recurrent geomagnetic activity is mainly restricted to high latitudes, providing further evidence for the presence of periodic auroral heating.

[34] The existence of periodic oscillations in the topside ionosphere further demonstrates the importance of periodic high-speed streams on the Earth's upper ionosphere. Including 9 day periodic modulation in the topside ionosphere associated with high-speed solar winds and coronal holes may aid in improving ionospheric weather prediction. Understanding this periodic modulation in the ionosphere linked to recurring solar wind forcing will be vital in future modeling of solar wind-magnetosphere-ionosphere-thermosphere coupling.

[35] **Acknowledgments.** Jing Liu thanks Jiuhou Lei for his valuable comments on the initial manuscript before submission. DMSP data were provided by the Center for Space Science at University of Texas at Dallas

(UT Dallas) and the U.S. Air Force. The geomagnetic indexes were obtained from World Data Center C2 for Geomagnetism in Kyoto, Japan. Solar wind data were downloaded from the Coordinated Data Analysis Web (CDAWEB) site. This research was supported by the National Natural Science Foundation of China (Grants 40725014 and 40804041) and a project supported by the Specialized Research Fund for State Key Laboratories. The work at UT Dallas was supported by NASA Grant NNX07AT82G.

[36] Robert Lysak thanks two anonymous reviewers for their assistance in evaluating the manuscript.

References

Blanc, M., and A. D. Richmond (1980), The ionospheric disturbance dynamo, *J. Geophys. Res.*, *85*, 1669–1686.

Bobova, V. P., and N. N. Stepanina (1994), Variations of the magnetic fields of the sun and the earth in 7–50 day periods, *Sol. Phys.*, *152*, 291–296, doi:10.1007/BF01473217.

Borovsky, J. E., and M. H. Denton (2006), Differences between CME-driven storms and CIR-driven storms, *J. Geophys. Res.*, *111*, A07S08, doi:10.1029/2005JA011447.

Burke, W. J., L. C. Gentile, and M. P. Hagan (2010), Thermospheric heating by high-speed streams in the solar wind, *J. Geophys. Res.*, *115*, A06318, doi:10.1029/2009JA014585.

Crooker, N. U., and E. W. Cliver (1994), Postmodern view of M-regions, *J. Geophys. Res.*, *99*, 23,383–23,390, doi: 10.1029/94JA02093.

Crowley, G., A. Reynolds, J. P. Thayer, J. Lei, L. J. Paxton, A. B. Christensen, Y. Zhang, R. R. Meier, and D. J. Strickland (2008), Periodic modulations in thermospheric composition by solar wind high speed streams, *Geophys. Res. Lett.*, *35*, L21106, doi:10.1029/2008GL035745.

Denton, M. H., J. E. Borovsky, R. M. Skoug, M. F. Thomsen, B. Lavraud, M. G. Henderson, R. L. McPherron, J. C. Zhang, and M. W. Liemohn (2006), Geomagnetic storms driven by ICME- and CIR-dominated solar wind, *J. Geophys. Res.*, *111*, A07S07, doi:10.1029/2005JA011436.

Donnelly, R. F., and L. C. Puga (1990), Thirteen-day periodicity and the center-to-limb dependence of UV, EUV, and X-ray emission of solar activity, *Sol. Phys.*, *130*, 369–390.

Fejer, B. G., and L. Scherliess (1997), Empirical models of storm time equatorial zonal electric fields *J. Geophys. Res.*, *102*, 24,047–24,056, doi:10.1029/97JA02164.

Field, P. R., and H. Rishbeth (1997), The response of the ionospheric F2-layer to geomagnetic activity: An analysis of worldwide data, *J. Atmos. Sol. Terr. Phys.*, *59*, 163–180.

Forbes, J. M., S. E. Palo, and X. Zhang (2000), Variability of the ionosphere, *J. Atmos. Sol. Terr. Phys.*, *62*, 685–693.

Fuller-Rowell, T. J., M. Codrescu, and P. Wilkinson (2000), Quantitative modeling of the ionospheric response to geomagnetic activity, *Ann. Geophys.*, *18*, 766–781, doi:10.1007/s00585-000-0766-7.

Gondhalekar, P. M. (1973), The behavior of the topside ionosphere during the magnetically disturbed conditions, *J. Atmos. Terr. Phys.*, *35*, 1293–1298.

Greenspan, M. E., W. J. Burke, F. J. Rich, W. J. Hughes, and R. A. Heelis (1994), DMSP F8 observations of the mid-latitude and low-latitude top ionosphere near solar minimum, *J. Geophys. Res.*, *99*, 3817–3826.

Harvey, K. L., and F. Recely (2001), Polar coronal holes during cycles 22 and 23, *Sol. Phys.*, *211*, 405–417.

Heelis, R. A., and W. R. Coley (2007), Variations in the low- and middle-latitude topside ion concentration observed by DMSP during superstorm events, *J. Geophys. Res.*, *112*, A08310, doi: 10.1029/2007JA012326.

Heelis, R. A., W. B. Hanson, and G. J. Bailey (1990), Distributions of the He^+ at middle and equatorial latitudes during solar maximum, *J. Geophys. Res.*, *95*, 10,313–10,320.

Hocke, K. (2008), Oscillations of global mean TEC, *J. Geophys. Res.*, *113*, A04302, doi:10.1029/2007JA012798.

Kil, H., L. J. Paxton, X. Pi, M. R. Hairston, and Y. Zhang (2003), Case study of the 15 July 2000 magnetic storm effects on the ionosphere-driver of the positive ionospheric storm in the winter hemisphere, *J. Geophys. Res.*, *108*(A11), 1391, doi:10.1029/2002JA009782.

Krieger, A. S., A. F. Timothy, and E. C. Roelof (1973), A coronal hole and its identification as the source of a high velocity solar wind stream, *Sol. Phys.*, *23*, 123.

Lei, J., J. P. Thayer, J. M. Forbes, E. K. Sutton, and R. S. Nerem (2008a), Rotating solar coronal holes and periodic modulation of the upper atmosphere, *Geophys. Res. Lett.*, *35*, L10109, doi:10.1029/2008GL033875.

Lei, J., J. P. Thayer, J. M. Forbes, E. K. Sutton, R. S. Nerem, M. Temmer, and A. M. Veronig (2008b), Global thermospheric density variations caused by high-speed solar wind streams during the declining phase of solar cycle 23, *J. Geophys. Res.*, *113*, A11303, doi:10.1029/2008JA013433.

Lei, J., J. P. Thayer, J. M. Forbes, Q. Wu, C. She, W. Wan, and W. Wang (2008c), Ionosphere response to solar wind high-speed streams, *Geophys. Res. Lett.*, *35*, L19105, doi:10.1029/2008GL035208.

Lei, J., J. P. Thayer, W. Wang, and R. L. McPherron (2010), Impact of CIR storms on thermosphere density variability during the solar minimum of 2008, *Sol. Phys.*, doi:10.1007/s11207-010-9563-y, in press.

Liang, M.-C., K.-F. Li, R.-L. Shia, and Y. L. Yung (2008), Short-period solar cycle signals in the ionosphere observed by FORMOSAT-3/COSMIC, *Geophys. Res. Lett.*, *35*, L15818, doi:10.1029/2008GL034433.

Liu, L., B. Zhao, W. Wan, S. Venkartraman, M. L. Zhang, and X. Yue (2007a), Yearly variations of global plasma densities in the topside ionosphere at middle and low latitudes, *J. Geophys. Res.*, *112*, A07303, doi:10.1029/2007JA012283.

Liu, L., W. Wan, X. Yue, B. Zhao, B. Ning, and M.-L. Zhang (2007b), The dependence of plasma density in the topside ionosphere on solar activity level, *Ann. Geophys.*, *25*(6), 1337–1343.

Liu, L., W. Wan, B. Ning, and M. L. Zhang (2009), Climatology of the mean TEC derived from GPS Global Ionospheric Maps, *J. Geophys. Res.*, *114*, A06308, doi:10.1029/2009JA014244.

Lomb, N. R. (1976), Least-squares frequency analysis of unequally spaced data, *Astrophys. Space Sci.*, *39*, 447–462.

Luan, X., W. Wang, A. Burns, S. Solomon, Y. Zhang, and L. J. Paxton (2010), Seasonal and hemispheric variations of the total auroral precipitation energy flux from TIMED/GUVI, *J. Geophys. Res.*, *115*, A11304, doi:10.1029/2009JA015063.

MacPherson, B., S. A. Gonzalez, G. J. Bailey, R. J. Moffett, and M. P. Sulzer (1998), The effects of meridional winds on the O^+-H^+ transition altitude over Arecibo, *J. Geophys. Res.*, *103*, 29,183–29,198.

Mlynczak, M. G., F. J. Martin-Torres, C. J. Mertens, B. T. Marshall, R. E. Thompson, J. U. Kozyra, E. E. Remsberg, L. L. Gordley, J. M. Russell, and T. Woods (2008), Solar-terrestrial coupling evidenced by periodic behavior in geomagnetic indexes and the infrared energy budget of the thermosphere, *Geophys. Res. Lett.*, *35*, L05808, doi:10.1029/2007GL032620.

Mursula, K., and B. Zieger (1996), The 13.5-day periodicity in the Sun, solar wind, and geomagnetic activity: The last three solar cycles, *J. Geophys. Res.*, *101*, 27,077–27,090.

Musman, S., and R. C. Altrock (1978), Recurrent geomagnetic disturbances and coronal holes as observed in Fe XIV l5303 A, *J. Geophys. Res.*, *83*, 4817–4822.

Nayar, S. R., V. S. Nair, V. N. Radhika, and K. Revathy (2001), Short-period features of the interplanetary plasma and their evolution, *Sol. Phys.*, *201*, 405–417, doi:10.1023/A:1017599621110.

Nerney, S., and S. T. Suess (2005), Stagnation flow in the thin streamer boundaries, *Astrophys. J.*, *624*, 378.

Neugebauer, M., E. Smith, A. Ruzmaikin, J. Feynman, and A. Vaughan (2000), The solar magnetic field and the solar wind: Existence of preferred longitudes, *J. Geophys. Res.*, *105*(A2), 2315–2324.

Pedatella, N. M., and K. M. Larson (2010), Routine determination of the plasmapause based on COSMIC GPS total electron content observations of the midlatitude trough, *J. Geophys. Res.*, *115*, A09301, doi:10.1029/2010JA015265.

Pedatella, N. M., J. Lei, J. P. Thayer, and J. M. Forbes (2010), Ionosphere response to recurrent geomagnetic activity: Local time dependency, *J. Geophys. Res.*, *115*, A02301, doi:10.1029/2009JA014712.

Pogoreltsev, A. I., A. A. Vlasov, K. Fröhlich, and C. Jacobi (2007), Planetary waves in coupling the lower and upper atmosphere, *J. Atmos. Sol. Terr. Phys.*, *69*, 2083–2101.

Qian, L., S. C. Solomon, and M. G. Mlynczak (2010), Model simulation of thermospheric response to recurrent geomagnetic forcing, *J. Geophys. Res.*, *115*, A10301, doi:10.1029/2010JA015309.

Rich, F. J., P. J. Sultan, and W. J. Burke (2003), The 27-day variations of plasma densities and temperatures in the topside ionosphere, *J. Geophys. Res.*, *108*(A7), 1297, doi:10.1029/2002JA009731.

Rishbeth, H. (1998), How the thermospheric circulation affects the ionosphere, *J. Atmos. Sol. Terr. Phys.*, *60*, 1385–1402.

Schwenn, R. (1983), Direct correlations between coronal transients and interplanetary disturbances, *Space Sci. Rev. 34*, 85–99.

Scargle, J. D. (1982), Studies in astronomical time series analysis. II. Statistical aspects of spectral analysis of unevenly spaced data, *Astrophys. J.*, *263*, 835–853.

Shugai, Y. S., I. S. Veselovskya, and L. D. Trichtchenko (2009), Studying correlations between the coronal hole area, solar wind velocity, and local magnetic indices in the Canadian region during the decline phase of cycle 23, *Geomagn. Aeron.*, *49*, 435–445.

Sojka, J. J., R. L. McPherron, A. P. van Eyken, M. J. Nicolls, C. J. Heinselman, and J. D. Kelly (2009), Observations of ionospheric heating during the passage of solar coronal hole fast streams, *Geophys. Res. Lett.*, *36*, L19105, doi:10.1029/2009GL039064.

Sultan, P. J., and F. J. Rich (2001), Determination of a proxy for F region meridional neutral winds using in situ satellite ion density measurements, *J. Geophys. Res.*, *106*, 21,033–21,038.

Svalgaard, L., and J. M. Wilcox (1975), Long term evolution of solar sector structure, *Sol. Phys.*, *41*, 461–475, doi:10.1007/BF00154083.

Temmer, M., B. Vršnak, and A. M. Veronig (2007), Periodic appearance of coronal holes and the related variation of solar wind parameters, *Sol. Phys.*, *241*, 371–383, doi:10.1007/s11207-007-0336-1.

Thayer, J. P., J. Lei, J. M. Forbes, E. K. Sutton, and R. S. Nerem (2008), Thermospheric Density oscillations due to periodic solar wind high-speed streams, *J. Geophys. Res.*, *113*, A06307, doi:10.1029/2008JA013190.

Tsurutani, B. T., W. D. Gonzalez, A. L. C. Gonzalez, F. Tang, J. K. Arballo, and M. Okada (1995), Interplanetary origin of geomagnetic activity in the declining phase of the solar cycle, *J. Geophys. Res.*, *100*(A11), 21,717–21,733.

Tsurutani, B. T., et al. (2006), Corotating solar wind streams and recurrent geomagnetic activity: A review, *J. Geophys. Res.*, *111*, A07S01, doi:10.1029/2005JA011273.

Tulasi Ram, S., J. Lei, S.-Y. Su, C. H. Liu, and W. S. Chen (2010), Dayside ionospheric response to recurrent geomagnetic activity during the extreme solar minimum of 2008, *Geophys. Res. Lett.*, *37*, L02101, doi:10.1029/2009GL041038.

Venkatraman, S., and R. Heelis (2000), Interhemispheric plasma flows in the equatorial topside ionosphere, *J. Geophys. Res.*, *105*, 18,457–18,464.

Vincent, R. A. (1990), Planetary and gravity waves in the mesosphere and lower thermosphere. *Adv. Space Res.*, *10*(12), 93–101.

Watanabe, S., K.-I. Oyama, and M. A. Abdu (1995), Computer simulation of electron and ion densities and temperatures in the equatorial *F* region and comparison with Hinotori results, *J. Geophys. Res.*, *100*(A8), 14,581–14,590.

Xiong, J., W. Wan, B. Ning, L. Liu, and Y. Gao (2006), Planetary wave type oscillations in the ionosphere and their relationship to mesospheric/lower thermospheric and geomagnetic disturbances at Wuhan (30.61N,114.51E), *J. Atmos. Sol. Terr. Phys.*, *68*, 498–508.

Zhang, Y., L. J. Paxton, and D. Morrison (2010), Auroral and thermospheric response to the 9 day periodic variations in the dayside reconnection rate in 2005, *Space Weather*, *8*, S07001, doi:10.1029/2009SW000559.

Zhao, B., W. Wan, L. Liu, X. Yue, and S. Venkatramn (2005a), Statistical characteristics of the total ion density in the topside ionosphere during the period 1996–2004 using empirical orthogonal function (EOF) analysis, *Ann. Geophys. 23*, 3615–3631.

Zhao, B., W. Wan, and L. Liu (2005b), Responses of equatorial anomaly to the October–November 2003 superstorms, *Ann. Geophys.*, *23*, 693–706.

R. A. Heelis, Hanson Center for Space Sciences, University of Texas at Dallas, 800 W. Campbell Rd., Richardson, TX 75080-3021, USA.

J. Liu, L. Liu, W. Wan, and B. Zhao, Institute of Geology and Geophysics, Chinese Academy of Sciences, Beijing 100029, China. (liul@mail.iggcas.ac.cn)